Applications in Energy and Combustion Science 13 (2023) 100114

Contents lists available at ScienceDirect

Applications in Energy and Combustion Science

journal homepage: www.sciencedirect.com/journal/applications-in-energy-and-combustion-science

Laminar burning velocity blending laws using particle imaging velocimetry

Yu Xie [a], Jinzhou Li [a], Junfeng Yang [a,*], Roger Cracknell [b]

[a] School of Mechanical Engineering, University of Leeds, Leeds LS2 9JT, United Kingdom
[b] Shell Global Solutions (UK), London SE1 7NA, United Kingdom

ARTICLE INFO

Keywords:
Laminar burning velocity
Particle imaging velocimetry
Blending laws

ABSTRACT

One of the most essential inherent characteristics of a combustible mixture is laminar burning velocity. Because of its relevance, many methods for measuring laminar flame velocity have been devised. One advanced procedure was used to derive laminar burning velocity in a constant volume vessel for blends of iso-octane and n-heptane/air mixtures in this study: particle imaging velocimetry. Based on a precise flow field with vectors, particle imaging velocimetry (PIV) provides highly accurate laminar burning velocities. The results of the PIV method were compared with Schlieren data and simulations based on detailed LLNL gasoline surrogate chemical kinetics. It was found that the measured laminar burning velocities using the PIV method were more consistent. To predict the laminar burning velocity of the binary mixture of primary reference fuel (PRF) investigated in this study, five blending laws were used and all of them demonstrated strong application and high accuracy. The Leeds *Q/k* law based on the variation curve of the heat release rate/reaction process was found to have a strong predictive capability as well.

1. Introduction

In spite of widespread electrification, there will still be a large number of vehicles with internal combustion engines beyond 2050. Achieving the goal of net zero, is also likely to require the defossilization of existing fuels [1,2] and the study of the combustion of gasoline and diesel components is as important as it has ever been. Single-component surrogates may be sufficient for simple purposes like determining combustion efficiency. For example, iso-octane is the most basic surrogate for gasoline fuel. Binary blends of gasoline primary reference fuels (PRFs) (i.e. iso-octane and n-heptane mixtures) have been commonly used as handy surrogates in studies mainly because of the direct connection with octane rating tests [3], although surrogates of increasing complexity are also proposed in the literature [4–5].

The laminar burning velocity is a crucial measure for assessing the burning property of homogenous fuel-air mixtures. The unstretched laminar burning velocity, u_l, is a key physico-chemical characteristic of a propagating flame that is determined by chemical reaction kinetics, exothermicity, and molecular transport mechanisms inside the reaction zone. This feature is used as a key input parameter in models of turbulent combustion and ignition limits [6]. It is particularly crucial for optimal combustor design since burn duration, power output, and efficiency are all tied to burning velocity predictions.

A variety of approaches (e.g. flat flame method, stagnation flame method and outwardly propagating spherical flame method) have been employed in the past to derive laminar burning velocities [7]. However, the constant volume vessel is the most versatile method of measuring laminar burning velocities [8], allowing burning velocity to be measured over a wide range of pressures and temperatures. Classically, the laminar flames are ignited at the center of a closed chamber by a spark when the unburned mixtures are stationary, afterwards, the history of the increasing pressure recorded by the pressure transducer (the so-called constant volume method) or the visual record of the expanding spherical flame before the pressure has increased significantly, as recorded by Schlieren ciné-photography or shadowgraphy (the so-called constant pressure method) could be adopted respectively in these methods to derive the unstretched laminar flame speed. While both strategies exist, researchers tend to choose one over the other, or are confined to a single method in particular circumstances. The measurement utilizing the constant volume method can also be impacted by the shape and size of the combustion vessel. Generally, pressure rather than burning velocity is directly measured, and therefore accurate equations are required to calculate the final results.

Two imaging techniques are employed for the constant pressure method to obtain the flame front: Schlieren ciné-photography (or shadowgraphy) technique [9] and Particle Imaging Velocimetry (PIV) technique [10]. The extraction of u_l using Schlieren ciné-photography

* Corresponding author.
E-mail address: J.Yang@leeds.ac.uk (J. Yang).

https://doi.org/10.1016/j.jaecs.2023.100114
Received 12 May 2022; Received in revised form 8 December 2022; Accepted 6 January 2023
Available online 7 January 2023

Nomenclature

a	number of moles of air that react with a mole of fuel
c	reaction progress variable
c_p	mean specific heat (J/kg/K)
k_u	thermal conductivity of unburned gas (J/m/K/s)
k_m	mean thermal conductivity (J/m/K/s)
L_u	unburned gasses Markstein length (mm)
m	mass (kg)
M_a	molecular masses of air
M_f	molecular masses of fuel
M_w	molecular mass
P	pressure (MPa)
Q	mass heat of reaction (J/kg)
r_{PIV}	flame radius obtained by PIV (mm)
r_u	flame radius defined as the isotherm = 365 K (mm)
R	radius of the spherical bomb (mm)
S_n	stretched flame speed (m/s)
t	time (s)
T	temperature (K)
$\widetilde{T}_a$	activation temperature based on u_l (K)
T_{al}	activation temperature based on $u_l\rho_u$ (K)
T_b	adiabatic burned gas temperature (K)
T_u	initial unburned fresh gas temperature (K)
u_g	maximum outwards gas velocity component normal to the flame front (m/s)
u_l	unstretched laminar burning velocity (m/s)
$u_{l,bl}$	unstretched laminar burning velocity of the blend (m/s)
u_n	stretched laminar burning velocity (m/s)
$\overline{x}$	mixture mole fraction
$\overline{x}_f$	fuel mole fraction
$\overline{x}_m$	mixture mass fraction
$\overline{x}_{mf}$	fuel mass fraction
Z	Zel'dovich number = $(T_a/T_b^2)(T_b - T_u)$

Greek symbols

α	flame stretch rate (1/s)
λ	burning velocity eigenvalue
γ_u	ratio of specific heat of unburned gas to burned gas
ρ_u	unburned gas density (kg/m^3)
ϕ	equivalence ratio

technique is based on the mass conversation method, which assumes flame adiabaticity or full equilibrium condition of the burned gasses, whereas in reality equilibrium requires a certain time and length scale to be attained [11], thereby making the results of burning velocities much less precise, particularly at low pressure. Using Schlieren ciné-photography technique, previous research showed that u_l of n-butanol/air mixtures at 0.1 MPa would be 4–11% lower than PIV measurement, with bigger discrepancies for the rich mixtures [10]. Furthermore, Direct Numerical Simulations [12] indicated that the uncertainty of burning velocities in highly radiating spherical explosion flames cannot be neglected based just on Schlieren measurements. It was shown that neglecting radiation in constant volume experiments could introduce errors, the magnitude of which depends on fuel type and initial conditions [13,14]. The PIV approach allows the laminar burning velocity to be calculated directly from the flame displacement speed and the unburned gas velocity ahead of the flame front. The PIV technique has been proved to be an efficient and accurate approach to measuring u_l of various hydrocarbon fuels [10,11,15,16].

The aforementioned classical methods have been widely employed to evaluate the flame propagation properties of the different components of gasoline surrogates. The laminar burning velocities of n-heptane, iso-octane, and toluene, as well as other PRF mixtures, have been measured under atmospheric conditions in [17]. Farrell et al. [18] investigated the laminar burning velocities of 45 hydrocarbons (C1-C4 alkanes, alkenes, and alkynes) in a constant volume combustion vessel at elevated temperature and pressure using the pressure rise technique (constant volume method). Taking advantage of simple operation, good imaging technology and high precision of Schlieren ciné-photography technique, Bradley et al. [19] studied the laminar burning velocities and Markstein lengths for n-heptane/iso-octane/air mixtures in a fan-stirred combustion vessel up to 1.0 MPa. Jerzembeck et al. [20] found that PRF (RON 84) and gasoline had experimentally identical laminar flame qualities at engine-relevant conditions. Mannaa et al. [21] projected normalised laminar burning velocity data onto a tri-component mixture space under a variety of experimental conditions in order to assign separate gasoline surrogates for different gasoline fuels with RONs of 70, 85, and 95. The results satisfactorily duplicate the burning rate characteristics of the gasoline fuels associated with these RONs under the various experimental situations studied. A multi-zone model was proposed to calculate burning velocity from pressure and Schlieren data obtained from a constant volume vessel [22].

One advantage of the PIV method with respect to Schlieren method is that it directly measures the laminar burning velocity without the assumption that the burned gas density at zero stretch rate is that of an adiabatic flame under equilibrium conditions. As an emerging technique, it has great potential for exploring the fundamental understanding of combustion research and improving the accuracy of burning velocity measurements. The aim of the present study is two-fold: first, to study the laminar burning velocity of mixtures of iso-octane and n-heptane, comparing different blending laws for predicting the laminar burning velocity of PRFs; second, to provide reasonable and accurate laminar burning velocity data using PIV technique (rather than traditional Schlieren photography).

2. Experimental apparatus

As illustrated in Fig. 1, a 380 mm-diameter spherical stainless-steel vessel with wide optical access through three pairs of orthogonal 150-mm-diameter windows was used [10]. The vessel has four electric-motor-driven fans that were primarily employed to guarantee that the reactants were well mixed before igniting in this study. To achieve the criteria, one electric heater (2 kW) was attached to the inner wall of the bomb to warm the vessel and mixture. A sheathed chromel-alumel thermocouple was used to monitor the gas temperature. A Kistler 701A, dynamic pressure transducer (calibrated to ±0.5% of full scale at 25.0 MPa) was used to detect pressures during an explosion. An imaging laser sheet of about 0.5 mm thick was generated by a double pulsed Nd: YAG laser (DM60–532-DH, Photonics Industries) with a wavelength of 532 nm and a series of lenses. The tracer particles (olive oil droplets with a diameter of about 1 μm, with a boiling temperature of about 570 K) [10], are injected into the flow with the assumption that they will travel in lockstep with the local velocity. A high-speed camera pointed perpendicular to the laser sheet captured a 12 bit picture pair of 768 × 768 pixels of the flow field and flame propagation. The detailed settings of PIV experiment are listed in Table 1. Additional details can be found in [10,23].

The full range mixtures of isooctane/n-heptane ratios in every 10% mole fraction were used for measuring the blending laminar burning velocities. Measurements of blending mixtures were made at the initial temperature = 360 K, initial pressure = 0.5 MPa and stoichiometric equivalence ratio ($\phi = 1$) for spherical explosion flames. The temperature of 360 K was chosen to ensure that iso-octane/n-heptane/air

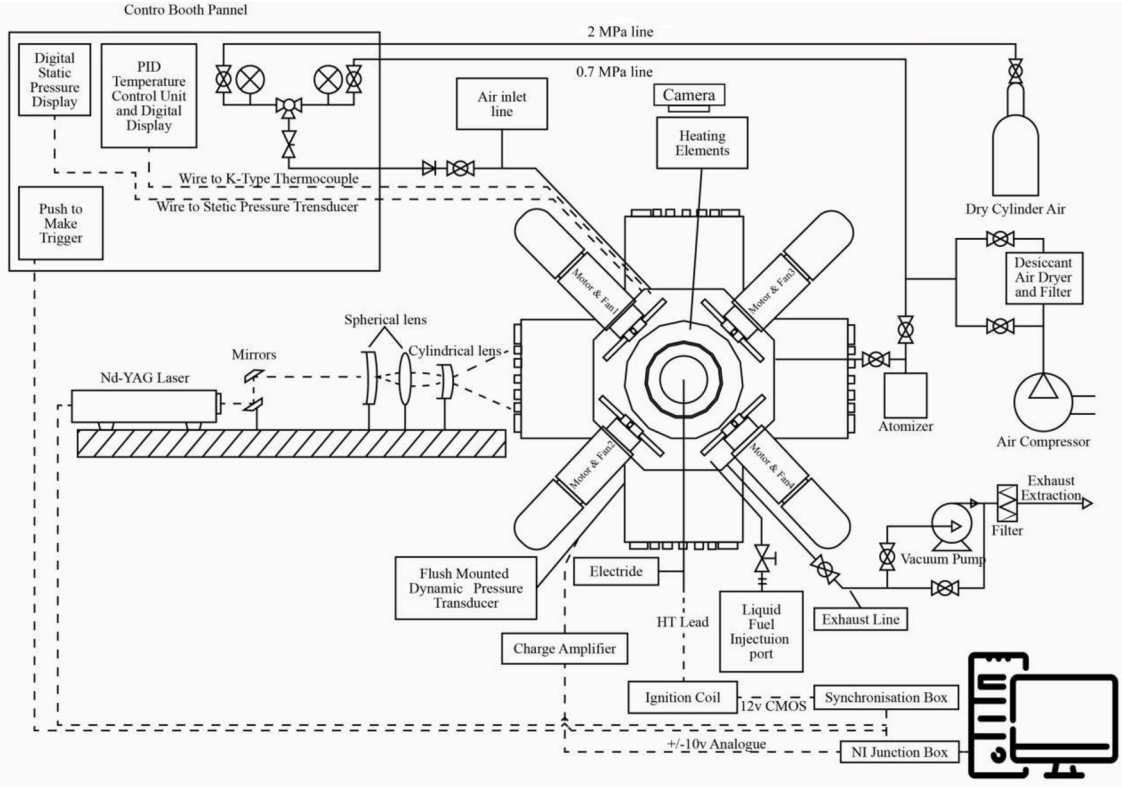

Fig. 1. Leeds MKII fan-stirred bomb with particle imaging velocimetry technique [23].

Table 1
Specifications of PIV setting.

Item	Value
Seeding	olive oil
Seeding size (μm)	1
Density(kg/m^3)	920
Boiling temperature (K)	570
Camera	Ultrahigh-Speed Phantom v2012
Resolution [Pixel]	768 × 768
Frame rate [Hz]	5k
Exposure time [μs]	20
Pixel size (mm/pixel)	0.22
Laser	DM60-532-DH
Laser color	Green
Laser type	Nd: YAG laser
Wavelength [nm]	532
Maximum output power [W]	120
Maximum output energy [mJ]	12
Pulse length[ns]	190
Pulse repetition rate [Hz]	1–30 k, 5 k used in this study
Beam diameter[mm]	3

mixtures were completely evaporated before combustion. The partial pressure method was used to prepare the air-fuel mixtures inside the combustion chamber. The minimal ignition spark energy (approximately 3 mJ) used to ignite the mixture with a central spark plug (provided by a 12 V transistorized automobile ignition coil) was used in all explosions. Three realisations of each experimental condition were used to ensure that the experiment is repeatable.

3. Calculations of laminar burning velocity from PIV technique

3.1. PIV technique

Fig. 2 shows the process of PIV post-processing method based on the computational software Dantec Dyamicstudio 5.1 [24] developed by Dantec Dynamics Company. The burned gas is presented by a black circle due to the evaporation of seeding particles, the grayish white region beyond the circle is illuminated by Mie scattering of seeding particles irradiated by a laser sheet. The addition of seeding particles suggested no significant differences in the combustion [23]. Using an image balancing tool in Dantec software, the flame edge was identified more clearly from the images by initially increasing the low-level brightness. The image balancing module corrects non-uniformities in light sheets that might impact the results of other analysis processes. Then the burned and unburned gas were distinguished using binarization tool in MATLAB R2019a [25]. Then, in binary pictures, the 'imfill' function was used to fill gaps and incoherent areas. The 'bwperim' function was used to find the perimeter of flame contour edges in a binary picture. A low pass filter was used to smooth the observed flame edges and remove any noise. The best fit circle to the flame edge and the matching flame radius, r_{PIV}, are then determined using the least squares technique.

Following the capture of pictures of the seeding particles by the PIV system, an assessment was carried out to determine the gas flow velocities. An adaptive algorithm known as the Adaptive PIV approach was employed within the Dantec software. This was an iterative and automated technique of computing velocity vectors based on seeding particle density and flow gradients. By establishing maximum and minimum size limitations, the proper interrogation area (IA) size was automatically established for each individual IA by the Adaptive PIV approach. The highest IA size was usually employed in the initial iteration. The placement and magnitude of vectors were defined by the minimal IA. This point was chosen to correspond with the edge of the minimum IA. The overlap of IA is often used with a typical value of 25% for the adaptive correlation method, the IA grid is set as: a maximum IA of 16 × 16 pixels, and a minimum IA of 8 × 8 pixels in this study, the more details are shown in [23]. The value of u_g (maximum outwards gas velocity component normal to the flame front) can be obtained from the gas vectors ahead of the flame front, which is also the rate of

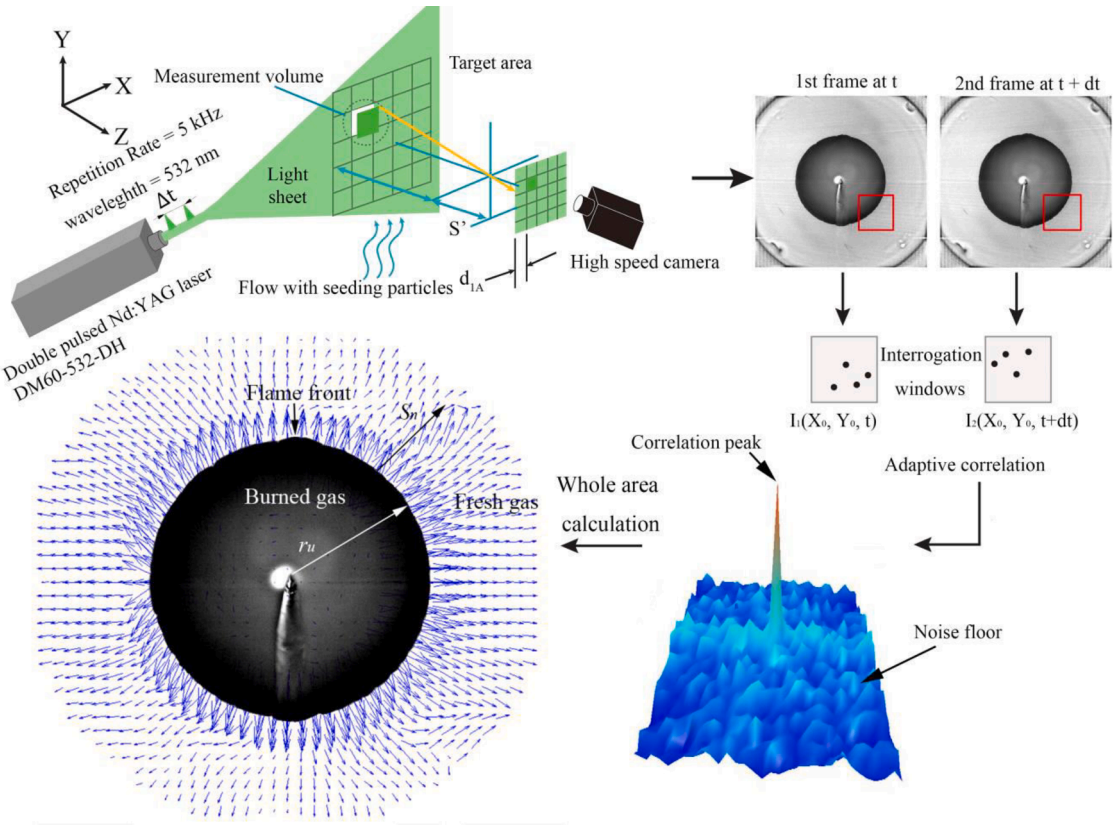

Fig. 2. 2D field calculation of PIV flame image and gas vectors using adaptive correlation.

entrainment of cold unburned gas by the flame front. The details of obtaining u_g are in [10,23].

PIV technique adopts the method of subtracting gas velocity from flame speed, using the following equation, the stretched laminar burning velocity, u_n, is given directly by the flame speed and the fresh gas velocity at the entrance of the flame front:

$$u_n = S_n - u_g \tag{1}$$

Here u_n is the stretched laminar burning velocity, S_n (dr_u/dt), is the stretched flame speed, r_u is the flame radius. r_u is calculated based on the assumption of a linear increase of temperature from unburned gas to burned gas:

$$r_u = r_{PIV} + \delta\left[\frac{T_P - (T_u + 5)}{T_b - (T_u + 5}\right] \tag{2}$$

where r_u, defined as the isotherm = 365 K (5 K above the initial temperature of the reactants), T_P is the seeding particle evaporation temperature in PIV technique (570 K). T_b is the adiabatic burned gas temperature (K), T_u is the unburned fresh gas temperature (K). Then the values of flame thickness δ were determined from the temperature profile of 1D freely propagating flame simulated using the Chemkin-Pro 19.2 [26] with detailed chemical kinetics [27].

The overall stretch rate, α, of a spherical explosion flame, of flame radius, r_u, is given by:

$$\alpha = \frac{1}{A}\frac{dA}{dt} = \frac{2}{r_u}\frac{dr_u}{dt} = \frac{2}{r_u}S_n \tag{3}$$

The unstretched laminar burning velocity, u_l, is extrapolated by the linear method [20]:

$$u_l = u_n + L_u\alpha \tag{4}$$

where L_u is the Markstein length relative to the unburned gasses (i.e. fresh gasses).

The extraction of u_l using Schlieren ciné-photography technique using the mass conversation method utilises the adiabatic values of both burned gas density and temperature with no inherent allowance for either strain rate changes in mean burned gas density, or those due to radiative energy loss. The PIV method does not need to make such constricting assumptions and the associated changes in the burning velocity are embodied in the measurements of S_n and u_g. Numerous studies have been conducted to investigate the radiation heat loss in laminar flames. Chen [28] used the mass conversation approach to show the relevance of radiation in lowering the unstretched laminar burning velocities for CH4/air mixtures. Along with the precise chemical kinetics and flow patterns, mathematical modeling of laminar flames must also take into account the effects of flame stretching and radiative energy loss or gain. But reductions in burning velocities due to radiative energy loss are less than 1% under near-stoichiometric conditions for heptane/air mixtures [29] and isooctane/air mixtures [10]. Consequently, radiation effects are not taken into account in this study.

4. Blending relationships and stoichiometry

4.1. Mixture compositions

The composition of a blend can be stated in a variety of ways, including mole fraction, mass fraction, volume fraction, and so on. When evaluating any blending law, a thorough grasp of such relationships and blend stoichiometry is essential. Before considering alternative blending laws, it is important to understand how the different ingredient mixtures, blends, and fuel amounts are specified. As a result, the composition of constituent mixtures must be expressed in terms of the value of ϕ. For one mole of fuel and a mole of air, the following equation is used:

$$\phi = \frac{1/a}{(1/a)_s} \tag{5}$$

Here, subscript s denotes stoichiometric condition.

As a result, one mole of a fuel-air combination consists of:

$$\left[\frac{1}{1+(1/\phi)/(1/a)_s}\right]_{\text{fuel}} + \left[\frac{(1/\phi)/(1/a)_s}{1+(1/\phi)/(1/a)_s}\right]_{\text{air}} = 1 \tag{6}$$

Then Eq. (6) can be simplified as:

$$\left[\frac{\phi}{\phi+a_s}\right]_{fuel} + \left[\frac{a_s}{\phi+a_s}\right]_{air} = 1 \tag{7}$$

The above is the basic mixing criterion. The following section shows the proportions of each component in the combination based on four measurement units: moles of fuel and air, moles of fuel, mass of fuel and air, mass of fuel, and liquid volume of fuel.

Consider one mole of a binary blend, where $\bar{x}_i$ refers to the fuel and air mole fraction of ith ingredient within the total moles of the blend. (fuel + air moles)/total moles). (e.g. $\bar{x}_1 + \bar{x}_2 = 1$):

$$\begin{aligned}\bar{x}_i &= \left[\left(\frac{\phi}{\phi+a_s}\right)_{fuel} + \left(\frac{a_s}{\phi+a_s}\right)_{air}\right]_i \\ &\left\{\sum_{i=1}^{n}\left[\left(\frac{\phi}{\phi+a_s}\right)_{fuel} + \left(\frac{a_s}{\phi+a_s}\right)_{air}\right]_i\right\}^{-1}\end{aligned} \tag{8}$$

The fuel mole percentage of the ith ingredient within the total fuel moles of the blend is stated as, $\bar{x}_{fi}$ for blends regarded only in terms of their fuel moles (fuel moles/total fuel moles):

$$\bar{x}_{fi} = \left(\frac{\phi\bar{x}}{\phi+a_s}\right)_{fuel,i}\left[\sum_{i=1}^{n}\left(\frac{\phi\bar{x}}{\phi+a_s}\right)_{fuel,i}\right]^{-1} \tag{9}$$

The mass-based equivalents of Eqs. (8) and (9) are easily determined using the following formula:

$$m = nM_w \tag{10}$$

where m represents mass, n is mole, M_w is molar mass.

As a result, the mass proportion of fuel and air in the ith ingredient within the overall mass of the blend (fuel + air mass)/total mass) is given by:

$$\begin{aligned}\bar{x}_{mi} &= \left[\left(\frac{\phi M_f}{\phi+a_s}\right)_{fuel} + \left(\frac{a_s M_a}{\phi+a_s}\right)_{air}\right]\bar{x}_i \\ &\left\{\sum_{i=1}^{n}\left[\left(\frac{\phi M_f}{\phi+a_s}\right)_{fuel} + \left(\frac{a_s M_a}{\phi+a_s}\right)_{air}\right]\bar{x}_i\right\}^{-1}\end{aligned} \tag{11}$$

The molecular masses of fuel and air are denoted by M_f and M_a, respectively. And, within the overall fuel mass of the blend, the fuel mass proportion of ith element is given by (fuel mass/total fuel mass):

$$\bar{x}_{mfi} = \left(\frac{\phi M_f\bar{x}}{\phi+a_s}\right)_{fuel,i}\left[\sum_{i=1}^{n}\left(\frac{\phi M_f\bar{x}}{\phi+a_s}\right)_{fuel,i}\right]^{-1} \tag{12}$$

4.2. Laminar burning velocity blending laws

4.2.1. Mole blending law

Payman and Wheeler [30] proposed the most seminal blending law. To get $u_{l,bl}$ of the blend, they employed the straightforward equation of weighting u_l of each constituent mixture by that of its mole fraction inside the blend:

$$u_{l,bl} = \sum_{i=1}^{n}(\bar{x}u_l)_i \tag{13}$$

Here, the mole fraction of the ith ingredient mixture within the total moles of the blend is denoted by $\bar{x}$.

4.2.2. Mass blending law

Van Lipzig et al. [31] studied the law of mixing based on mass, so that the u_l of each component mixture is weighted according to the mass fraction in the mixture to obtain the $u_{l,bl}$ of the mixture:

$$u_{l,bl} = \sum_{i=1}^{n}(\bar{x}_m u_l)_i \tag{14}$$

Here, the mass fraction of the ith ingredient mixture within the overall mass of the blend is denoted by $\bar{x}_m$.

4.2.3. Le Châtelier based blending law of Di Sarli

Using the CHEMKIN PREMIX code and the GRI kinetic mechanism 3.0, Di Sarli and Benedetto [32] developed a Le Châtelier (LC) rule-like formula:

$$u_{l,bl} = \frac{1}{\sum_{i=1}^{n}\left(\frac{\bar{x}_f}{u_l}\right)_i} \tag{15}$$

where $\bar{x}_f$ denotes the fuel mole fraction of the ith constituent within the total fuel moles of the blend.

4.2.4. Activation temperature blending law of Hirasawa

Firstly, Spalding made a pioneering mathematical analysis of laminar combustion velocity [33,34]. The following is his expression for mass burning rate:

$$u_l\rho_u = \left[\frac{k_u\int_0^1 R(c)dc}{\lambda(T_b-T_u)c_p^2}\right]^{0.5} \tag{16}$$

where k_u is the thermal conductivity of unburned gas, c_p, the mean specific heat, ρ_u is the density of unburned gas, λ is the burning velocity eigenvalue, and c is the reaction progress variable, $\int_0^1 R(c)dc$ is the volumetric heat release rate source term, more details can be found in [35,36].

Eq. (16) can also be expressed as [36]:

$$\left(Qc_p/k_u\right)^{0.5}u_l\rho_u = \left[\frac{\int_0^1 R(c)dc}{\lambda}\right]^{0.5} \tag{17}$$

where Q is the heat of reaction of unit mass of the mixture.

The volumetric heat release rate source term $\int_0^1 R(c)dc$ can be written as [37]:

$$\int_0^1 R(c)dc = \int_0^1 S(c)\exp(-T_a/T)dc \tag{18}$$

where $dc/dT = (T_b - T_u)^{-1}$, it can be shown:

$$\int_0^1 R(c)dc = \int_0^1 S(c)\left[\frac{T_a}{T^2}(T_b-T_u)\right]^{-1}d\exp(-T_a/T) \tag{19}$$

All heat release happens at T_b, according to the asymptotic assumption of large activation energy [38], Eq. (19) can be expressed as [36]:

$$\int_0^1 R(c)dc = \int_0^1 S(1)\left[\frac{T_a}{T_b^2}(T_b - T_u)\right]^{-1}\exp(-T_a/T_b) = (\mathrm{S}(1)/\mathrm{Z})\exp(-T_a/T_b) \tag{20}$$

where Z is the Zel'dovich number $= (T_a/T_b^2)(T_b - T_u)$.

And then Eq. (16) becomes:

$$u_l\rho_u = \left[\frac{k_m S(1)\exp(-T_a/T_b)}{0.5Z(T_b - T_u)c_p^2}\right]^{1/2} \tag{21}$$

where k_m is the mean thermal conductivity, and then:

$$u_l\rho_u = \exp - \left[(T_a/2T_b) - \ln\left(\frac{k_m S(1)}{0.5Z(T_b - T_u)c_p^2}\right)^{1/2}\right] \tag{22}$$

And then a commonly utilised expression in asymptotic analyses can be obtained:

$$u_l\rho_u = \exp(-T_{al}/2T_b) \tag{23}$$

where $T_{al} = T_a - 2T_b\ln\left(\frac{k_m S(1)}{0.5Z(T_b-T_u)c_p^2}\right)^{1/2}$, and the laminar burning mass flow has an activation temperature of T_{al}.

A slightly different activation temperature, $\widetilde{T}_a$, dependent on the sole u_l alone rather than $u_l\rho_u$, with the following was proposed by Hirasawa et al. [37] for modifying the Eq. (23):

$$u_l = \exp(-\widetilde{T}_a/T_b) \tag{24}$$

As a result, the activation temperature of the blend, $\widetilde{T}_{a,bl}$ is:

$$\widetilde{T}_{a,bl} = \sum_{i=1}^{n}[\overline{x}T_b\ln(u_l)]_i \tag{25}$$

Finally, the laminar burning velocity of the blend, $u_{l,bl}$, is calculated as:

$$u_{l,bl} = \exp\left(\frac{-\widetilde{T}_a}{T_b}\right)_{bl} \tag{26}$$

4.2.5. Q/k blending law of Leeds

The Leeds blending law is based on Eq. (17), Spalding's equation for the mass rate of combustion, and mass weighting of the integrated reaction rate terms of the constituent fuel/air mixtures. To one side, the macro parameters u_l, Q, k_u, c_p, and ρ_u are used, while the remaining indicate a reactivity measure by presenting the volumetric heat release rate profile through the flame:

$$u_l\rho_u\left(\frac{Qc_p}{k_u}\right)^{0.5} = \left[\frac{\int_0^1 R(c)dc}{\lambda}\right]^{0.5} \tag{27}$$

Then Eq. (27) yields:

$$\left[u_l\rho_u\left(\frac{Qc_p}{k_u}\right)^{0.5}\right]_{bl} = \left[\frac{\int_0^1 R(c)dc}{\lambda}\right]_{bl}^{0.5} = \sum_{i=1}^{n}\overline{x}_{mi}\left[\frac{\int_0^1 R(c)dc}{\lambda}\right]_i^{0.5} \tag{28}$$

Eventually, The Leeds blending law is obtained by applying fractional mass weighting to the respective macro parameters$(Qc_p/k_u)^{0.5}u_l\rho_u$:

$$\left[u_l\rho_u\left(\frac{Qc_p}{k_u}\right)^{0.5}\right]_{bl} = \sum_{i=1}^{n}\left[xu_l\rho_u\left(\frac{Qc_p}{k_u}\right)^{0.5}\right]_i \tag{29}$$

The Leeds blending law assumes that the u_l of any mixture ultimately depends on the volumetric heat release rate curve through the flame. From the perspective of the individual thermal conductivity of different mixtures, it will have a higher sensitivity to significantly different mixtures, which has been verified before [36].

Throughout this study, Chemkin-Pro 19.2 [26] with detailed chemical kinetics [27] was used to get all values such as Q and so on for all mixtures.

5. Results and discussions

5.1. Pressure measurement

The pressure traces for pure iso-octane with and without seeding particles are presented in Fig. 3. The partial pressure method was used to prepare the mixtures, and the amount of 0.02 MPa of air with seeding particles was used in this study. The results of pressure traces suggest the impact of seeding particles on the combustion process is negligible when the particle pressure of seeding particles is 0.02 MPa. This conclusion is not only applicable for iso-octane but also for other hydrocarbon fuels [10,23].

Pressure traces of iso-octane and n-heptane/air blending mixtures over different mole fractions are presented in Fig. 4. All of the pressure traces follow a similar pattern, starting at 0.5 MPa and peaking at 3.5 MPa, and then leveling off. What stands out here is that pure iso-octane/air mixture takes the longest time to go from the initial pressure value to the peak pressure value, while pure n-heptane/air mixture takes the shortest time, and other blends are evenly distributed between two pressure curves.

5.2. Laminar burning velocities from PIV method

The significant advantage of the PIV approach is the direct measurement of unburned gas velocity ahead of flame front u_g, and flame propagation speed S_n, which yields the stretched burning velocity, u_n from Eq. (1). By plotting stretched burning velocity against the stretch rate and with a linear extrapolation of the resulting curve to zero stretch ($\alpha = 0$), the unstretched burning velocity, u_l, can be obtained from the intercept (as shown in Fig. 5). The extrapolation is carried out with the selected data range overseen at every stage to ensure a realistic fit and application only within the stable regime of the flame growth. Above the curves on the left side is the unstable region and on the right side is the spark-affected region. Moreover, the nonlinear extrapolation method was proposed and introduced for extrapolating the unstretched flame speeds [39–42]. According to the results presented in [11,43], the nonlinear method and the linear method are quite close to each other under stoichiometric conditions for iso-octane/air mixtures. Hence, the nonlinear extrapolation method was not adopted here.

Variations of u_l for stoichiometric blends of n-heptane and iso-octane

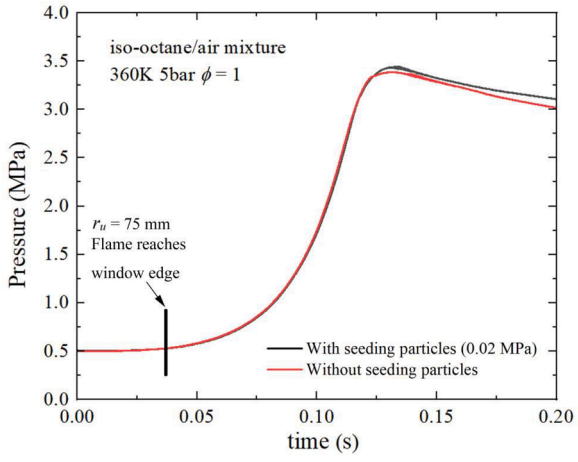

Fig. 3. Pressure traces for a stoichiometric isooctane/air mixture at the pressure of 0.5 MPa, the temperature of 360 K and $\phi = 1.0$ with varying seeding particle amounts.

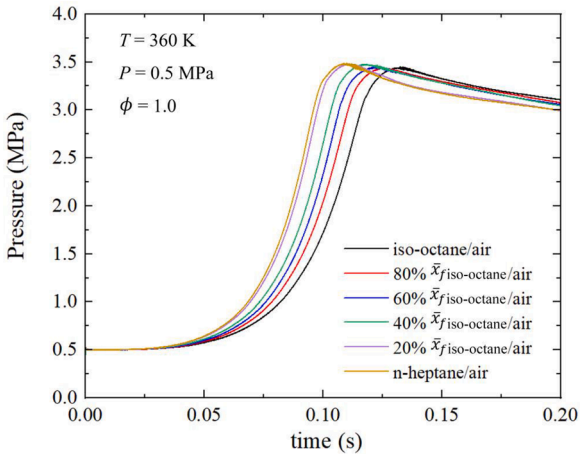

Fig. 4. Evolutions of the pressure inside the vessel during the combustion of isooctane and n-heptane/air mixtures initially at the pressure of 0.5 MPa, the temperature of 360 K and $\phi = 1.0$.

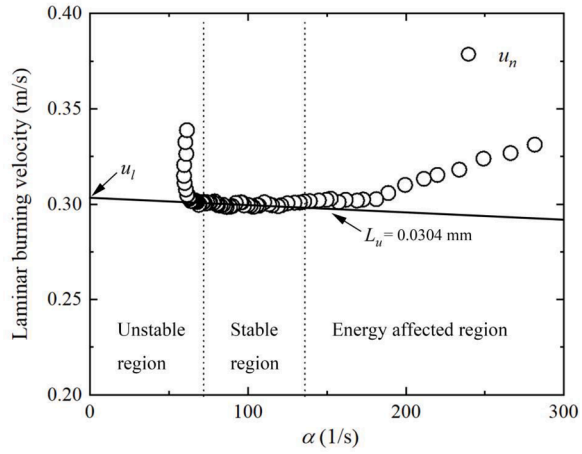

Fig. 5. Variations of stretched laminar burning velocities against flame stretch rate α of stoichiometric pure isooctane/air mixture under the initial pressure of 0.5 MPa, temperature of 360 K.

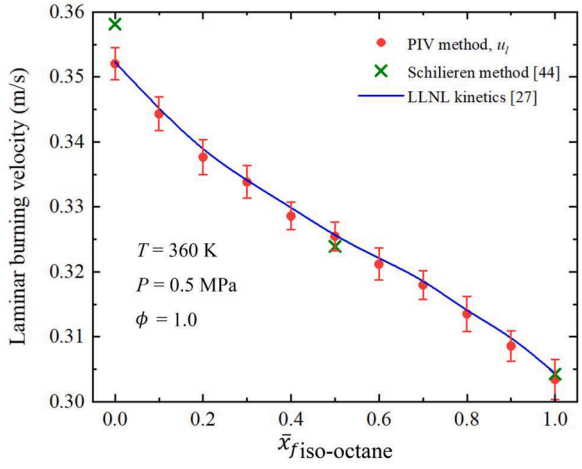

Fig. 6. Variations of laminar burning velocities against $\bar{x}_{fiso-octane}$ for the blend of isooctane and n-heptane/air mixtures, also with data from Schlieren method data [44] and LLNL detailed kinetics [27] using Chemkin-Pro 19.2. The standard deviation method is used for calculating uncertainties represented by error bars [45].

at different mole percentages are plotted in Fig. 6. In addition to PIV laminar burning velocities, comparisons are also made with Schlieren data [44] for blends of n-heptane and iso-octane/air mixtures on the same Leeds combustion bomb. Furthermore, the laminar burning velocities of PRFs are calculated using LLNL detailed chemical kinetic mechanisms of gasoline surrogate mixtures [27] to verify the experimental results and are plotted in Fig. 6. The comparison supports the view that the Schlieren approach does not provide the same high level of accuracy as the PIV method. The results using PIV method are more self-consistent with those calculated using LLNL detailed chemical kinetics than those using Schlieren method.

5.3. *Blending laws for laminar burning velocities*

Five blending laws are adopted in this study based on the laminar burning velocities calculated from the PIV method, as mentioned in Section 4.2. For Leeds Q/k blending law based on Spalding's expression for the mass rate of burning, this applies the fractional mass weighting to the separate term $((Qc_p/k_u)^{0.5}u_l\rho_u)$. The values of $(Qc_p/k_u)^{0.5}$ are calculated and plotted against $\bar{x}_{fiso-octane}$ for the blend of iso-octane and n-heptane/air mixtures in Fig. 7. It can be clearly seen that it increases linearly with $\bar{x}_{fiso-octane}$.

Predicted values of $u_{l,bl}$ for blends of stoichiometric iso-octane and n-heptane/air mixtures using five previously mentioned blending laws are compared with the experimentally measured values of u_l, using PIV technique in Fig. 8. What is gratifying is that five blending laws all show good prediction ability for iso-octane and n-heptane/air blends. Specifically, for iso-octane and n-heptane/air mixtures, the prediction accuracy of five blending laws in laminar burning velocity measurement is less than 0.6%. They underestimated laminar burning velocity in high iso-octane percentages while overestimating laminar burning velocity in high n-heptane percentages for the most time. The mole blending law ($\bar{x}$) makes the poorest forecast. Unexpectedly, the law of mole fraction $\bar{x}$ is not as good as the law of mass fraction $\bar{x}_m$. This can be found in methane and hydrogen blends as well [36]. The LC method, in comparison to other laws, takes the reciprocal form and is the only way to from the perspective of the fuel mole fraction of the ith condition within the total fuel moles of the blend ($\bar{x}_f$), which seems more reasonable than the mole fraction of the ith condition mixture within the total mole of the blend including air ($\bar{x}$). The mass blending law comes next. Leeds Q/k law is the second best law. This is understandable given the fact that it includes more variables. The Q/k law is also based on the mass blending law ($\bar{x}_m$). The mass weighting technique is enhanced based on the exothermic rate and specific heat of the constituent mixture. $\widetilde{T}_a$ law is the best prediction

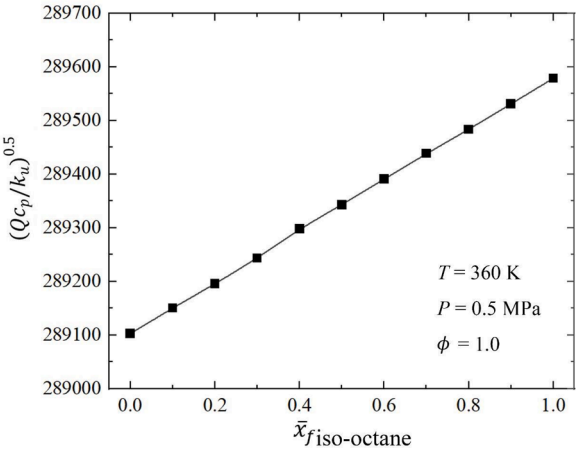

Fig. 7. Variations of $(Qc_p/k_u)^{0.5}$ against $\bar{x}_{fiso-octane}$ for the blend of isooctane and n-heptane/air mixtures at the initial pressure of 0.5 MPa, the temperature of 360 K and $\phi = 1.0$.

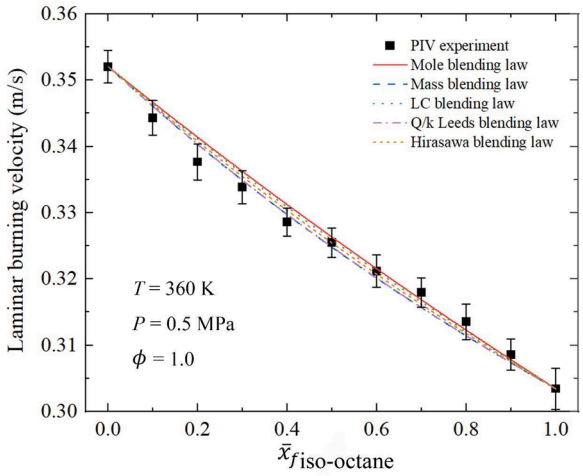

Fig. 8. Predicted and measured values of u_l for stoichiometric isooctane and n-heptane/air mixtures, as a function of $\overline{x}_{iso-octane}$. For each blending law, distinct curves represent predicted values. Experimental values with error bars are shown by black solid square symbols.

law. This is based on mole fraction weighting ($\overline{x}$), which is applying the activation temperature of blend on it.

6. Conclusion

Laminar burning velocity measurements have been made for PRF components in a constant volume vessel using the particle imaging velocimetry (PIV). The unique PIV technique is able to directly derive the burning velocity from the flame speed and the unburned gas velocity ahead of the flame front. In addition, all measured laminar burning velocities were compared with predicted data calculated using LLNL kinetic simulations. The results bear this out and show that PIV measurements provide values of unstretched which are more self-consistent than Schlieren method. From theoretical considerations, the PIV is superior to the other techniques (e.g. Schlieren method) that necessitate the chemical equilibrium assumption.

Five blending laws were employed to predict the laminar burning velocities of the binary mixture of the primary reference fuel (PRF) explored in this work. All blending laws demonstrate good application and high accuracy for this type of mixture from the standpoint of commercial prediction. Theoretically, through the changing curve of the heat release rate/reaction process, the Leeds *Q/k* law has the most robust theoretical basis, which translates into predictive capability.

Declaration of Competing Interest

The authors declare that they have no known competing financial interests or personal relationships that could have appeared to influence the work reported in this paper.

Data availability

Data will be made available on request.

Acknowledgments

Yu Xie acknowledges China Scholarship Council and University of Leeds for a joint PhD scholarship (CSC202008350141). Jinzhou Li thanks SHELL Global Solutions (UK) for offering a partially funded PhD scholarship.

References

[1] Balthasar F, Mikulic I, Kolbeck A, Wilbrand K, Cracknell R, Rijken K, Warnecke W. Pathways to meet renewable energy targets in transport. In: Proceedings of the 43rd international vienna motor symposium, 27–29 April; 2022. Vienna (Austria).
[2] Xie Y, Wei Z, Zhou T, Zhen H, Liu Z, Huang Z. Combustion characteristics of small laminar flames in an upward decreasing magnetic field. Energies 2021;14(7):1969.
[3] Gorbatenko I, Bradley D, Tomlin AS. Auto-ignition and detonation of n-butanol and toluene reference fuel blends (TRF). Combust Flame 2021;229:111378.
[4] Sarathy SM, Farooq A, Kalghatgi GT. Recent progress in gasoline surrogate fuels. Prog Energy Combust Sci 2018;65:67–108.
[5] Gail S, Cracknell RF, Poulet B, Lovett G, Festa A, Shankar V, Büttgen RD, Heufer KA. THIP: a new TPRF-like fuel surrogate development approach to better match real fuel properties. Fuel 2021;286:119395.
[6] Metghalchi M, Keck JC. Burning velocities of mixtures of air with methanol, isooctane, and indolene at high pressure and temperature. Combust Flame 1982; 48:191–210.
[7] Faghih M, Chen Z. The constant-volume propagating spherical flame method for laminar flame speed measurement. Sci Bull 2016;61(16):1296–310.
[8] Rallis CJ, Garforth AM, Steinz JA. Laminar burning velocity of acetylene-air mixtures by the constant volume method: Dependence on mixture composition, pressure and temperature. Combust Flame 1965;9(4):345–56.
[9] Xie Y, Morsy ME, Li J, Yang J. Intrinsic cellular instabilities of hydrogen laminar outwardly propagating spherical flames. Fuel 2022;327:125149.
[10] Bradley D, Lawes M, Morsy ME. Flame speed and particle image velocimetry measurements of laminar burning velocities and Markstein numbers of some hydrocarbons. Fuel 2019;243:423–32.
[11] Varea E, Modica V, Vandel A, Renou B. Measurement of laminar burning velocity and Markstein length relative to fresh gases using a new postprocessing procedure: application to laminar spherical flames for methane, ethanol and isooctane/air mixtures. Combust Flame 2012;159(2):577–90.
[12] Jayachandran J, Zhao R, Egolfopoulos FN. Determination of laminar flame speeds using stagnation and spherically expanding flames: molecular transport and radiation effects. Combust Flame 2014;161(9):2305–16.
[13] Movaghar A, Lawson R, Egolfopoulos FN. Radiation effects in confined spherically expanding flames: application to C_5-C_{10} flames at engine-relevant conditions. Proc Combust Inst 2021;38(2):2195–203.
[14] Hesse R, Berger L, Bariki C, Hegetschweiler MJ, Linteris GT, Pitsch H, Beeckmann J. Low global-warming-potential refrigerant CH_2F_2 (R-32): integration of a radiation heat loss correction method to accurately determine experimental flame speed metrics. Proc Combust Inst 2021;38(3):4665–72.
[15] Dong Y, Vagelopoulos CM, Spedding GR, Egolfopoulos FN. Measurement of laminar flame speeds through digital particle image velocimetry: mixtures of methane and ethane with hydrogen, oxygen, nitrogen, and helium. Proc Combust Inst 2002;29(2):1419–26.
[16] Balusamy S, Cessou A, Lecordier B. Direct measurement of local instantaneous laminar burning velocity by a new PIV algorithm. Exp Fluids 2011;50(4):1109–21.
[17] Sileghem L, Alekseev VA, Vancoillie J, Nilsson EJK, Verhelst S, Konnov AA. Laminar burning velocities of primary reference fuels and simple alcohols. Fuel 2014;115:32–40.
[18] Farrell JT, Johnston RJ, Androulakis IP. Molecular structure effects on laminar burning velocities at elevated temperature and pressure. SAE Trans 2004:1404–25.
[19] Bradley D, Hicks RA, Lawes M, Sheppard CGW, Woolley R. The measurement of laminar burning velocities and Markstein numbers for iso-octane–air and iso-octane–n-heptane–air mixtures at elevated temperatures and pressures in an explosion bomb. Combust Flame 1998;115(1–2):126–44.
[20] Jerzembeck S, Peters N, Pepiot-Desjardins P, Pitsch H. Laminar burning velocities at high pressure for primary reference fuels and gasoline: experimental and numerical investigation. Combust Flame 2009;156(2):292–301.
[21] Mannaa O, Mansour MS, Roberts WL, Chung SH. Laminar burning velocities at elevated pressures for gasoline and gasoline surrogates associated with RON. Combust Flame 2015;162(6):2311–21.
[22] Marshall SP, Taylor S, Stone CR, Davies TJ, Cracknell RF. Laminar burning velocity measurements of liquid fuels at elevated pressures and temperatures with combustion residuals. Combust Flame 2011;158(10):1920–32.
[23] Morsy MEMH. Studies of laminar and turbulent combustion using particle image velocimetry. University of Leeds; 2019. Doctoral dissertation.
[24] Dantec Dynamics. Dynamic studio user's guide. Denmark: Skovlunde; 2013.
[25] MATLAB. Natick, Massachusetts: The MathWorks Inc; 2018. 9.7. 0.1190202 (R2019b).
[26] ANSYS reaction design: chemkin Pro 19.2, San Diego, 2019.
[27] Mehl M, Pitz WJ, Westbrook CK, Curran HJ. Kinetic modeling of gasoline surrogate components and mixtures under engine conditions. Proc Combust Inst 2011;33(1): 193–200.
[28] Chen Z. On the accuracy of laminar flame speeds measured from outwardly propagating spherical flames: methane/air at normal temperature and pressure. Combust Flame 2015;162(6):2442–53.
[29] Santner J, Haas FM, Ju Y, Dryer FL. Uncertainties in interpretation of high pressure spherical flame propagation rates due to thermal radiation. Combust Flame 2014; 161(1):147–53.
[30] Payman W, Wheeler RV. The composition of gaseous fuels in relation to their utilisation. Fuel Sci Pract 1922;1:185–96.
[31] Van Lipzig JPJ, Nilsson EJK, De Goey LPH, Konnov AA. Laminar burning velocities of n-heptane, iso-octane, ethanol and their binary and tertiary mixtures. Fuel 2011; 90(8):2773–81.

[32] Di Sarli V, Di Benedetto A. Laminar burning velocity of hydrogen–methane/air premixed flames. Int J Hydrogen Energy 2007;32(5):637–46.
[33] Spalding DB. Mixing rule for laminar flame speed. Fuel 1956;35(3):347–51.
[34] Spalding DB. Predicting the laminar flame speed in gases with temperature-explicit reaction rates. Combust Flame 1957;1(3):287–95.
[35] Bradley D, Habik SED, El-Sherif SA. A generalisation of laminar burning velocities and volumetric heat release rates. Combust Flame 1991;87:245–336.
[36] Bradley D, Lawes M, Mumby R. Burning velocity and Markstein length blending laws for methane/air and hydrogen/air blends. Fuel 2017;187:268–75.
[37] Hirasawa T, Sung CJ, Joshi A, Yang Z, Wang H, Law CK. Determination of laminar flame speeds using digital particle image velocimetry: binary fuel blends of ethylene, n-butane, and toluene. Proc Combust Inst 2002;29(2):1427–34.
[38] Al-Mughanam T, Bradley D, Lawes M, Mumby R. Burning velocity blending laws for methane/air and hydrogen/air blends. In: Proceedings of the 25th international colloquium on the dynamics of explosions and reactive systems; 2015.
[39] Kelley AP, Law CK. Nonlinear effects in the extraction of laminar flame speeds from expanding spherical flames. Combust Flame 2009;156(9):1844–51.
[40] Wu F, Liang W, Chen Z, Ju Y, Law CK. Uncertainty in stretch extrapolation of laminar flame speed from expanding spherical flames. Proc Combust Inst 2015;35(1):663–70.
[41] Jiang Y, Xu H, Ma X, Bao X, Wang B. Laminar burning characteristics of 2-MTHF compared with ethanol and isooctane. Fuel 2017;190:10–20.
[42] Huo J, Yang S, Ren Z, Zhu D, Law CK. Uncertainty reduction in laminar flame speed extrapolation for expanding spherical flames. Combust Flame 2018;189:155–62.
[43] Halter F, Tahtouh T, Mounaïm-Rousselle C. Nonlinear effects of stretch on the flame front propagation. Combust Flame 2010;157(10):1825–32.
[44] Mumby RD. Experimental characterisation of fuel blends. University of Leeds; 2016. Doctoral dissertation.
[45] Zhang P, Zsély IG, Papp M, Nagy T, Turányi T. Comparison of methane combustion mechanisms using laminar burning velocity measurements. Combust Flame 2022;238:111867.